Non-Nominal Troposphere Reassessment for Meeting CAT II/III with MC/MF GBAS

Alizé Guilbert

Non-Nominal Troposphere Reassessment for Meeting CAT II/III with MC/MF GBAS

Alizé Guilbert, *TELECOM/SIGNAV Laboratory – ENAC, Toulouse, France*

BIOGRAPHY

Alizé GUILBERT is a French PhD student. She received in 2012 an Engineer Diploma from the Ecole Nationale Aviation Civile (ENAC) in Toulouse, France with a specialization in Aeronautical Telecommunications. She is currently doing a PhD in the SIGNAV laboratory at the ENAC for the SESAR (Single European Sky Air traffic management Research) project (WP15.3.7) since April 2013. Her subject is *the Development of Processing Models for Multi-Constellation/Multi-frequency (MC/MF) GBAS.*

ABSTRACT

In Civil Aviation, to meet the long term goal of greater capacity, services must be expanded to provide more reliable, robust approach and landing operations in all weather conditions. This could be achieved globally by using modernized navigation systems. This paper relates to the development of the Multi-Constellation (MC) and Multi-Frequency (MF) Ground Based Augmentation System (GBAS) within the SESAR Framework Work Package 15.3.7. It deals also with the performance improvements obtainable for CAT II/III precision approaches, the most stringent operation currently defined.

Several challenges and key issues must be solved including those related to atmospheric modelling. Previous work principally undertaken at Ohio University [1] [2] [3] highlighted the need to consider the troposphere as a possible source of failure. GBAS activities in Europe have followed the approach of validating the protection levels, which includes treating the combined threat relating to ionospheric and tropospheric gradients. Therefore the tropospheric failure should be bounded by validating that the combination of atmospheric errors does not exceed the assumed models.

However, there are a number of arguments for revisiting this topic and specifically addressing the tropospheric threat. Firstly, recent observations [4], reported at last ICAO NSP (International Civil Aviation Organisation – Navigation System Panel) meeting, showed unexpected atmospheric behavior. The source could be related to a non-modelled behavior of the troposphere. Even if the range errors induced by this phenomenon are not significant compared to those due to ionospheric gradients, the combination of these “tropospheric” gradients with ionospheric gradients could impact integrity and continuity.

Secondly, in the advent of dual-frequency GBAS, the ionosphere may feasibly be removed through the Ionosphere-Free (I-Free) smoothing technique. In this case, the main contributor to the atmospheric error will come from the tropospheric delay. Under such a scenario, the troposphere threat model must be defined and a means for bounding the potential errors derived.

This paper presents an initial analysis with the aim of evaluating the impact of non-nominal troposphere on VPL for different scenarios. The goal of this comparison is to ascertain the extent to which the proposed tropospheric bounding methodology increases the VPLs used at the aircraft.

Finally, this paper has initiated the process of assessing the impact of modelling the non-nominal troposphere on GBAS VPLs. Indeed a new methodology is proposed and seems to improve performance in terms of availability while respecting some constraints on a low data requirements for the VDB transmission.

INTRODUCTION

In the scope of the SESAR Work Package 15.3.7 several research threads are being undertaken to improve the performance of MC/MF GBAS to support CAT II/III precision approaches.

Several challenges and key issues must be solved including those related to atmospheric modelling. Previous work undertaken at Ohio University [1] [2] [3] highlighted the need to consider the troposphere as a possible source of failure. GBAS activities in Europe have followed the approach of validating the protection levels, which includes treating the combined threat relating to ionospheric and tropospheric gradients. Therefore the tropospheric failure should be bounded by validating that the combination of atmospheric errors does not exceed the assumed models.

However, there are a number of arguments for revisiting this topic and specifically addressing the tropospheric threat. Firstly, recent observations, reported at last ICAO NSP meeting [4], showed unexpected atmospheric behavior. These observations have been confirmed by the

FAA (Federal Aviation Administration) and Boeing and have shown that significant spatial gradients with no link to ionosphere activity are likely to appear mainly during warm and sunny days. The source could be related to a non-modelled behavior of the troposphere. Even if the range errors induced by this phenomenon are around 9 cm and are not significant compared to those due to ionospheric gradients, the combination of these "troposphere" gradients with ionospheric gradients could lead to missed detection or false detection of the ground subsystem's ionospheric monitor, thus impacting integrity and continuity.

Secondly, in the advent of dual-frequency GBAS, the ionosphere may feasibly be reduced significantly through the ionosphere-free smoothing technique. Under such a scenario, the troposphere threat model must be defined and a means for bounding the potential errors derived. One could argue that in all cases, each error source should be independently bounded and as such the possibility of gross errors due to the troposphere should be evaluated further, at least in the European region.

As a result of these needs, WP15.3.7 contains a task to analyze European meteorological data and models to better select and parameterize the threat model for the European region. In the initial study presented here, the threat as outlined in the U.S at Ohio University [3] is taken as input and the impact upon availability is assessed, determining an ideal protection level bound under these assumptions.

After a first part dealing with a brief introduction of the Nominal Troposphere and in order to understand the impact of non-nominal troposphere this paper will present the bounding concept as the Stanford University did in [5] [6] [7].

The model chosen for the non-nominal differential tropospheric delay is detailed in a dedicated part of this paper. Then simulations were run to check the impact of this delay on Vertical Protection Level (VPL) for several scenarios with the existing methodology. Different data will be analysed in this report with some comparison with results obtained by Ohio University.

Finally, in order to meet the requirements for the worst performing aircraft, lower Vertical Alert Limits (VALs) may be required which could impact availability. Under such conditions, it would be beneficial to utilize a tropospheric bounding methodology. That is why, the last part of this paper is dedicated to a new proposed methodology and its results analysis in terms of availability performances for both Single Frequency (SF) and Dual Frequency (DF) cases. The next steps of this study should focus on further developing a solution which requires low data transmitted for computing a smaller bound in the protection level domain and reassessing the model parameterization.

NOMINAL TROPOSPHERE

For both SF and DF with I-free smoothing technique, differential residual error due to the tropospheric delays are expressed as computed in [8] as follows:

$$\delta J = J^A - \left(J^G + t_{AZ}\dot{J}^G\right) \tag{1}$$

Where J is the tropospheric delay, t_{AZ} represents the time between the modified time of correction generation t_Z and the time of application at the airborne receiver. The notation $\blacksquare^G$ is used for parameters relating to the ground receivers and $\blacksquare^A$ for those relating to the airborne receiver and $\dot{\blacksquare}$ defines the linear derivative.

In order to address the 2nd-order temporal effects of the nominal troposphere errors, they may be decomposed into spatial and temporal components.

$$\delta J = \underbrace{J^A(t_A) - J^G(t_A)}_{spatial} + \underbrace{J^G(t_A) - \left(J^G(t_G) + t_{AZ}\dot{J}^G\right)}_{temporal} \tag{2}$$

It is currently under investigation within SESAR WP 15.3.7 as to whether $\dot{J}^G$ can be considered as a constant over the period of three smoothing windows. If so the residual differential error due to the troposphere will contain only a spatial component.

It is expected that the tropospheric delay variation is likely to be very linear in which case the difference: $J^G(t_A) - \left(J^G(t_G) + t_{AZ}\dot{J}^G\right)$ should be small, maybe negligible. So, only the spatial component remains which may be decomposed into horizontal and vertical components. The vertical component which arises from the height difference between ground station and aircraft is corrected using the standardized nominal model given in [9]. The horizontal component had been neglected within the standardized models. Horizontal gradients will be treated as non-nominal tropospheric events in this paper, even though minor such gradients have been observed more frequently than previously thought. [4]

OVER-BOUNDING AND INFLATION CONCEPTS

In order to understand the impact of non-nominal troposphere we have to present the bounding concept [6] [7]. It is not practical to completely remove all non-zero mean components (biases) in the pseudorange corrections. These error sources must be over-bounded and using Gaussian model with a standard deviation hypothesized to be conservative. That is why the concept of a $VPL_{Composite}$ was introduced, where the bounded errors and noisy errors are treated separately:

$$VPL_{Composite} = VPL_N + VPL_B \tag{3}$$

Where VPL_N is the VPL component that bounds the existing sources of error currently overbounded by a Gaussian distribution and VPL_B is the VPL component that arises from the non-zero biases, such as caused by non-nominal tropospheric error.

The previous formula (3) can be derived for each ranging sources i:

$$VPL_{Composite,i} \approx Kffmd \times S_{vert,i} \times \sigma_{N,i} + VPL_{B,i} \quad (4)$$

Where

$$VPL_{B,i} = |S_{vert,i}\mu(i)| \quad (5)$$

With μ(i) defined as the ranging bias for the satellite i in meters (out of the N number of visible satellites), $S_{vert,i}$ is the vertical component of the appropriate geometry matrix for the satellite i, $Kffmd$ is the fault-free missed detection multiplier and $\sigma_{N,i}$ is the standard deviation of the error source i noise only in meters.

Then, VPL-B can be evaluated with the following expression:

$$VPL_B = \sum_{i=1}^{N} VPL_{B,i} = \sum_{i=1}^{N} |S_{vert,i}\mu(i)| \quad (6)$$

And so $VPL_{Composite}$ can be approximated (as described in [7]) for all ranging source as:

$$VPL_{Composite} \approx Kffmd \times \sqrt{\sum_{i=1}^{N} |S_{vert,i}{}^2 \times \sigma_{N,i}{}^2|} + VPL_B \quad (7)$$

The equivalent bounding or inflated VPL may be expressed as:

$$VPL_{inflated} \approx Kffmd \times \sqrt{\sum_{i=1}^{N} |S_{vert,i}{}^2 * \sigma_{inflated,i}{}^2|} \quad (8)$$

Where $\sigma_{inflated,i}$ is the net sigma which includes the necessary inflation.

The $VPL_{Composite}$ can be seen as the "ideal" VPL and the $VPL_{inflated}$ as the user VPL or the current VPL.
Integrity is ensured by setting:

$$VPL_{Composite} \leq VPL_{inflated} \quad (9)$$

So that means that the inequality $\sigma_{N,i} < \sigma_{inflated}$ is required

In order to be conservative, the assumption that VPL_B considers the worst case (conspiring biases in our case) is made.

So the maximum value for VPL_B is defined by:

$$VPL_B max = \sum_{i=1}^{N} |S_{vert,i} \times \mu_{max}| \quad (10)$$

Where μ_{max} is the maximum ranging bias on all satellites.

According to [1] [2] it has been shown that VPL_B can be bounded and so its maximum $VPL_B max$ by:

$$VPL_B max \leq \mu_{max}\sqrt{N}\, VDOP \quad (11)$$

This $VPL_{Composite}$ aspect can be explained in the position domain by the following Figure 1 for each ranging source i:

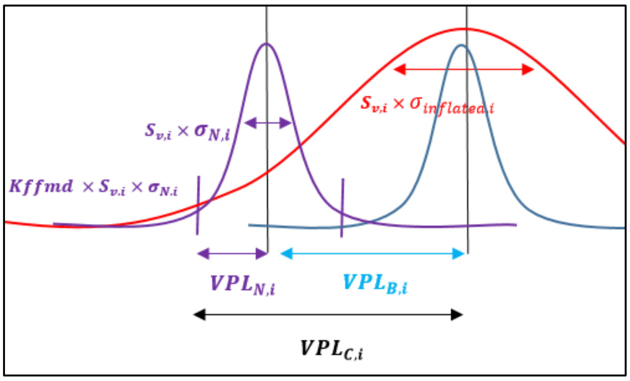

Figure 1 - VPL Composite concept

In order to have a clearer figure, $S_{v,i}$ represents the $S_{vert,i}$ variable and $VPL_{C,i}$ refers to the $VPL_{Composite}$ for the ranging source i.

The equation (9) explained above, expresses the need to define a protection level with an inflated standard deviation that is at least as large as the composite VPL.

EXISTING METHODOLOGY

Non-Nominal Troposphere Modelling

The model chosen for the non-nominal differential tropospheric delay, is the "Wall model" following [3]. As noted above, validation of this choice and further investigation into the European tropospheric threat is planned within 15.3.7. After discussions with partners and colleagues at Ohio University [10], alternative models such as the wedge, duct or along-wall models were neglected. These assumptions will be verified as part of the planned real data analysis.

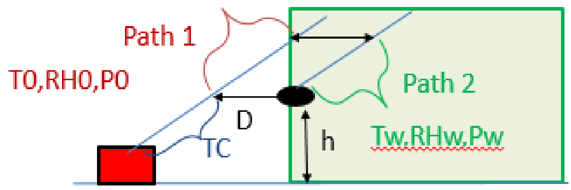

Figure 2 - Weather Wall Model to the right of the Ground Station

In Figure 2, when the signal to the GBAS ground facility leaves the weather wall (Path 1), it experiences different conditions (T0,P0,RH0) than the signal to the user that is located beyond the wall limit (Path 2) with conditions (Tw, RHw, Pw). In this case the wall is represented to the right of the aircraft but it could equivalently also be on the left with no loss of generality. This assumption is valid if the vertical tropospheric correction models both nominal and non-nominal vertical gradients.

Existing Proposition to Bound Non-Nominal Troposphere within GAST C/D framework

The existing proposal for dealing with non-nominal troposphere use the following methodology [7] [3]:

- *Bounding biases with Absolute Bias Approach (conspiring biases)* [7]

That assumes the same bias for all satellites: μ_{max}

- *Converting this bound to a standard deviation.*

It represents the bounding for non-nominal tropospheric standard deviation $\sigma_{non\_nom\_tropo}$
This can be achieved by using the formula (11) explained above and by seeing $VPL_B max \approx Kffmd \times VDOP \times \sigma_{non\_nom\_tropo}$ as it is also shown in details in [1] [2]

$$\sigma_{non\_nom\_tropo} = \frac{\mu_{max}\sqrt{N}}{K_{ffmd}} \quad (12)$$

- *Ensuring integrity with the Relative Inflation Concept* [7]

In this case σ_{vig} is inflated with $\sigma_{non\_nom\_tropo}$ which is transmitted to the A/C by making the root mean square between both values in order to form an inflated value : $\sigma_{vig\_inflated}$

$$\sigma_{vig\_inflated} = \sqrt{\sigma_{vig}^2 + \sigma_{non\_nom\_tropo}{}^2} \quad (13)$$

This Relative Inflation Concept is the simplest sigma inflation approach which makes the assumption that biases are proportional to the sigma for each ranging source. This concept is described in details in [7]

- *Implementing inflated $\sigma_{vig\_inflated}$ at the A/C* into

$$\sigma_{iono} = F_{pp} \times \sigma_{vig\_inflated} \times (x_{air} + 2\tau v_{air}) \quad (14)$$

- *Computing $VPL_{inflated}$ at the A/C*

Protection Levels are computed with the new σ_{iono} by the "traditional" way (without modifying VPL computation)

ANALYSIS

The initial analysis assesses the following VPLs:

- The VPL computed without non-nominal troposphere component (without non-zero mean bias) that is to say VPL_N
- The $VPL_{Composite}$ computed by adding the exact value of VPL_N and VPL_B
- The $VPL_{inflated}$ which is the VPL computed with the inflation methodology

The goal of this comparison is to ascertain the extent to which the proposed tropospheric bounding methodology increases the VPLs used at the aircraft in case of SF.

Processing Options and Parameters

The following model parameters are utilized in this analysis:

- Model implemented using Modified Hopfield Model from [11] (this differs from the studies by Ohio University [2] [3] as it captures better the vertical profile of the troposphere)
- The maximum number of tracked satellites by the airborne receiver is N=12 for GPS (24 for GPS+GAL) [5] (this differs from the value N=6 (and 12 respectively) as selected by Ohio University [3] in order to select the worst case N). Results obtained for N=6 for GPS and N=12 for GPS+GAL are presented in the appendix.
- D_{TH} is defined as the distance between the Ground Station and the Runway threshold. Then, two tests were performed with regards to the Ground Facility siting of D_{TH}=5km [12] and 10km instead of 1km employed in [3]
- A worst case mapping function is determined when determining the inflation in σ_{vig} (not 5° as taken in [3])
- The nominal weather conditions are defined with parameters: T0=15°C, P0=1023.25hPa and RH0=50%. The temperature lapse rate is set to -6.5K/km.
- The Wall weather conditions are defined with parameters: Tw=26°C, Pw=1023.25hPa and RHw=100%. The temperature lapse rate is also set to -6.5K/km.

Standard Deviations Determination

For determining the $\sigma_{non-nom-tropo}$, two curves were plotted on the same Figure 3: The lower one (in blue) represents the wall model non-nominal troposphere standard deviation from Equation (12) as a function of distance to the GBAS ground station. The upper curve (in red) represents the residual ionospheric uncertainty due to spatial decorrelation of the $\sigma_{non-nom-tropo}$ value. The goal is to overbound the non-nominal troposphere standard deviation so the value of $\sigma_{non-nom-tropo}$ is needed to be found numerically, selecting the minimum value which bounds the $\sigma_{non-nom-tropo}$ curve in blue.

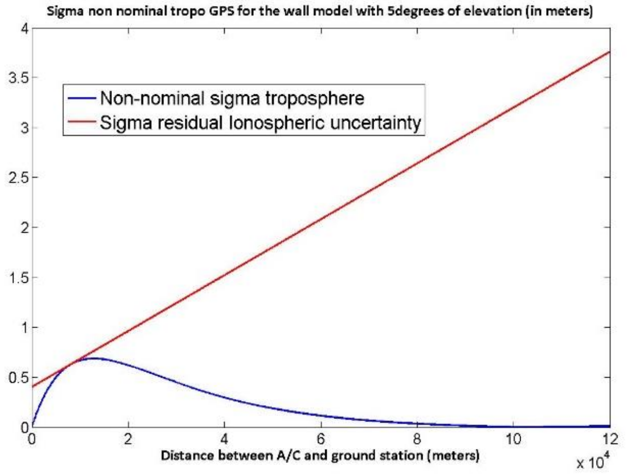

Figure 3 - Example of Bound of Non-Nominal Troposphere using the Residual Iono Uncertainty due to Spatial Decorrelation

In order to see the influence of the inflation of sigma on the VPL computation, Table 1 represents $\sigma_{non-nom-tropo}$ and $\sigma_{vig\_inflated}$ as a function of N and D_{TH} for comparison of different scenarios (Results obtained for N=6 for GPS and N=12 for GPS+GAL are presented in the Appendix).They were determined by using the Equation (13) with the nominal value of $\sigma_{vig} = 4mm/km$ and the methodology explained by the Figure 3.

	D_{TH} = 5km	D_{TH} = 10km
N=6	$\sigma_{non-nom-tropo}$ = 8.0mm/km $\sigma_{vig\_inflated}$ = 8.94mm/km	$\sigma_{non-nom-tropo}$ = 9.9mm/km $\sigma_{vig\_inflated}$ = 10.68mm/km
N=12	$\sigma_{non-nom-tropo}$ = 11.2mm/km $\sigma_{vig\_inflated}$ = 11.89mm/km	$\sigma_{non-nom-tropo}$ = 13.8mm/km $\sigma_{vig\_inflated}$ = 14.37mm/km
N=24	$\sigma_{non-nom-tropo}$ = 15.9mm/km $\sigma_{vig\_inflated}$ = 16.40mm/km	$\sigma_{non-nom-tropo}$ = 19.5mm/km $\sigma_{vig\_inflated}$ = 19.91mm/km

Table 1 - $\sigma_{non-nom-tropo}$ and $\sigma_{vig\_inflated}$ for different cases

The value obtained in [3] an with the equation (13) is:

- $\sigma_{non-nom-tropo}$ = 5.0mm/km for GPS constellation and D_{TH}=1km

  → $\sigma_{vig\_inflated} = 6{,}4031\ mm/km$

So by taking the parameter assumptions defined in the previous section, $\sigma_{vig\_inflated}$ of 11.89 mm/km was found instead of 6.4031 mm/km (as presented in [3]) with the D_{TH} of 5km and the GPS constellation chosen. This has an important impact on availability and thus suggests the existing proposition from Ohio University is more conservative than first determined.

Results

Simulations were run to check the impact of non-nominal troposphere on VPL for the following scenarios:

- 4 locations: Seattle Airport, Anchorage Airport, Miami Airport and an Airport located at a Latitude 0.
- GPS and GPS + GAL constellations
- D_{TH} =5km and D_{TH}=10km
- Five key points along the approach
  - Distance from A/C to Runway Threshold : D=20NM,
  - D=10NM
  - Altitude of A/C h=200ft,
  - h =100ft and
  - h=0ft.

Simulations were processed over 24 hours in the case of GPS and 10 days in the case of GPS + GALILEO, with a time resolution of 10seconds. In this report, the results for Seattle Airport and for an altitude of Aircraft h=200ft, are presented.

On the Figure 4, Figure 5, Figure 6 and Figure 7, different results are represented:

- **$VPL_{inflated}$ with non-nominal troposphere computed with the inflation methodology**
- **$VPL_{Composite}$ computed by adding the exact value of VPL_N and VPL_B**
- **VPL_N representing VPL without non-nominal troposphere**

Ultimately, if the tropospheric threat is considered significant enough to be bounded separately, the intention is to derive a means to bound the resulting error whilst keeping the data transmission load low.

For D_{TH} = 5km

In Figure 4, the different VPLs presented above are represented for the GPS constellation only and with a distance from ground station to runway threshold (D_{TH}) of 5km.

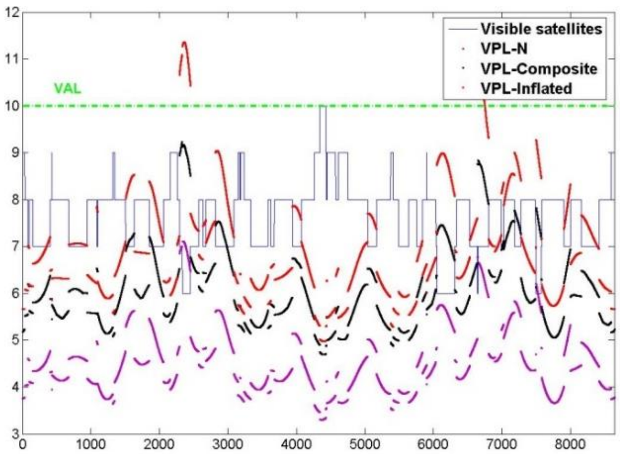

Figure 4 - VPLs with D_{TH}=5km for GPS constellation only

By analyzing this Figure 4, the following inequality is verified:

$$VPL_{inflated} > VPL_{Composite} > VPL_N \qquad (15)$$

Also by seeing the Vertical Alert Limit (VAL) (set to 10m), the remark that for some epochs $VPL_{inflated}$ is above to VAL can be made and this can clearly impact availability. In the Figure 5, the different VPLs presented above are represented for the GPS and Galileo constellations with a distance from ground station to runway threshold (D_{TH}) of 5km.

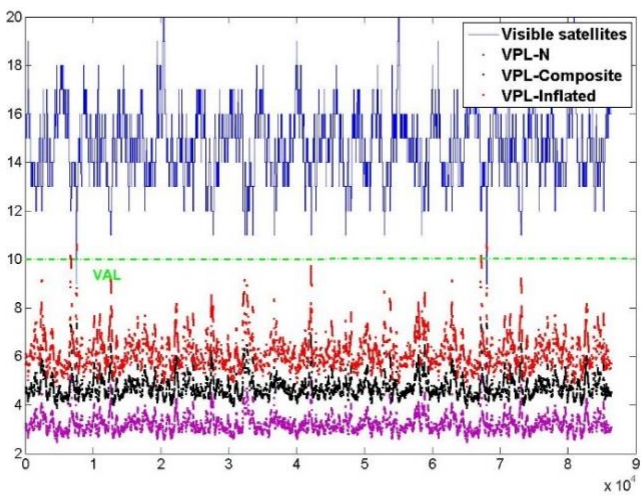

Figure 5- VPLs with D_{TH}=5km for GPS + GAL constellations

In the previous Figure 5, same results and conclusions as for Figure 4 can be made.

<u>For D_{TH}=10km</u>

In the Figure 6, the different VPLs presented above are represented for the GPS constellation only with a distance from ground station to runway threshold (D_{TH}) of 10km.

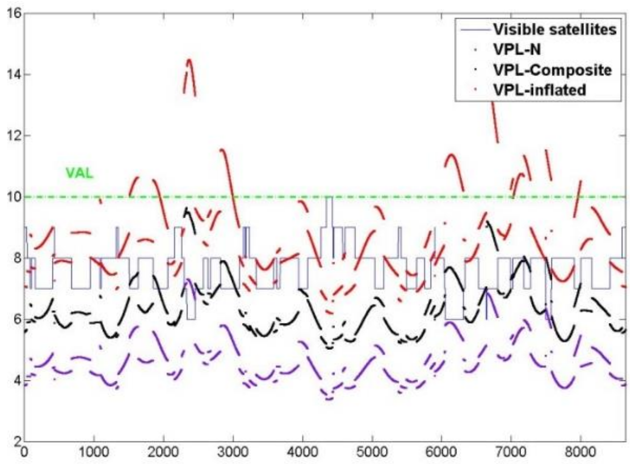

Figure 6 - VPLs with D_{TH}=10km for GPS constellation only

By looking at Figure 6, the inequality (15) is still verified. The level of VPLs appears more important for D_{TH} =10km than D_{TH}=5km.

Furthermore, cases where $VPL_{inflated}$ is larger than VAL are more numerous than for D_{TH}=5km.That means that for a larger D_{TH}, the availability is more impacted.

In Figure 7, the different VPLs presented above are represented for the GPS and Galileo constellations with a distance from ground station to runway threshold (D_{TH}) of 10km.

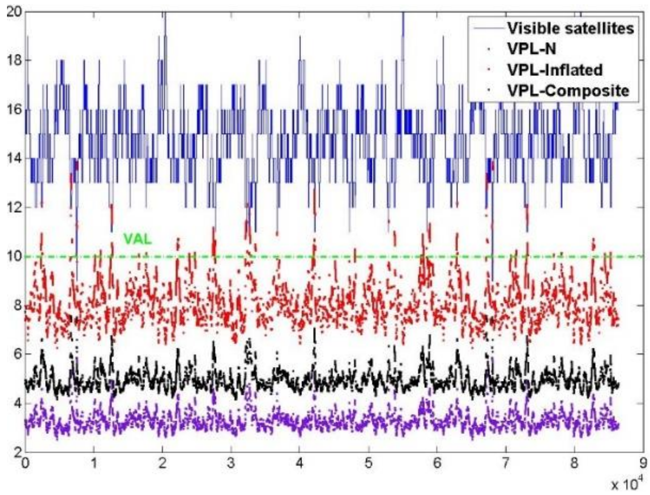

Figure 7 - VPLs with D_{TH}=10km for GPS + GAL constellations

In Figure 7, the same conclusions as for the GPS constellation case (Figure 6) is made concerning the validity of the inequality (15) and the level of VPLs.

But in this case of Dual Constellation GPS and Galileo, the difference between the VPL inflated (in red) and the VPL composite (in black) is more important. This leads to the conclusion that the methodology used is too conservative and finding a closer bound in the protection level domain appears feasible.

Furthermore, in the case of DF with I-Free smoothing technique, this methodology cannot be used anymore for dealing with the troposphere threat because the ionosphere component will be completely removed and no sigma parameter will therefore exist.

PROPOSED METHODOLOGY

The proposed methodology relies on the Modified Hopfield Model (MHM) [11] explained above to compute tropospheric delays and on the fact that that they depends on satellite elevations and distances from Ground Station to Aircraft. In this part of the work, the assumption that D_{TH}= 5km according SARPs [12] is made. This value defines the largest distance between Ground Station and runway threshold.

In fact, the first phase of the study was to compute a table representing tropospheric delays for sets of satellite elevations bin with a width of 5°, from 0° to 90° and for distances between ground station and aircraft varying from 300m up to 30km with different steps according to how far aircraft is. In this case, tropospheric delays are represented from 300m to 1km with a step of 100m then from 1km to 8km with a step of 500m and from 8km to 30km with a step of 1km.

The second phase was to take, for each elevation bin of 5°, the maximum value of tropospheric delays over distances. 18 values which can be called μ_{max} are obtained. It differs from the existing methodology because there is not only one value of μ_{max}.

Then, VPL_{PM1} is computed the same way as the previous $VPL_{Composite}$ as explained by the equation (7).
Finally, several curves are plotted in order to compare this methodology with others as done in the previous section.

Results

Simulations were processed over 24 hours in the case of GPS and 10 days in the case of GPS + GALILEO, with a time resolution of 10 seconds. This analysis was realized for all the five key points along the approach, as presented previously in this paper.

But in order to compare with previous results presented on Figure 4 and Figure 5, results for Seattle Airport and for an altitude of Aircraft h=200ft, are presented.

On the Figure 8 and Figure 9 different results are represented:

- **$VPL_{inflated}$ with non-nominal troposphere computed with the inflation methodology**
- **$VPL_{Composite}$ computed by adding the exact value of VPL_N and VPL_B**
- **VPL_N representing VPL without non-nominal troposphere**
- **VPL_{PM1} computed with the new proposed methodology**

In Figure 8, the different VPLs presented above are represented for the GPS constellation with a distance from ground station to runway threshold (D_{TH}) of 5km.

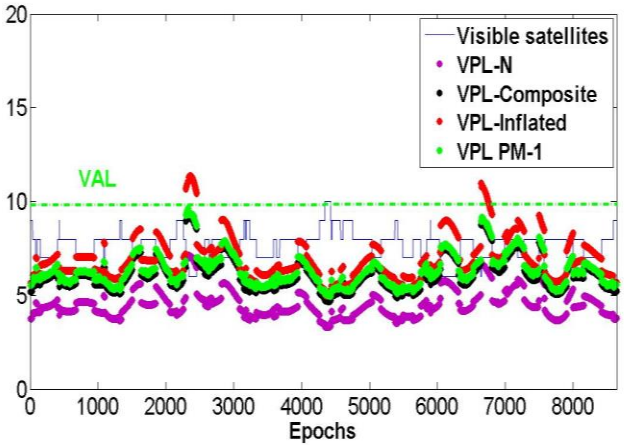

Figure 8 - VPLs with D_{TH}=5km for GPS constellation only

In the previous Figure 8, integrity is ensured because the following inequality is verified:

$$VPL_{Composite} \leq VPL_{PM1} \quad (16)$$

Furthermore, the availability is improved compared to the existing inflation methodology. Indeed the following inequality is obtained:

$$VPL_{PM1} \leq VPL_{inflated} \quad (17)$$

The level of VPL with this new methodology represented by the green line is closer to the $VPL_{Composite}$ (black line) than with the inflation methodology (red line). That is why for the GPS constellation case, an improvement in term of performance is made.

In the Figure 9, the different VPLs presented above are represented for the GPS and Galileo constellations with a distance from ground station to runway threshold (D_{TH}) of 5km.

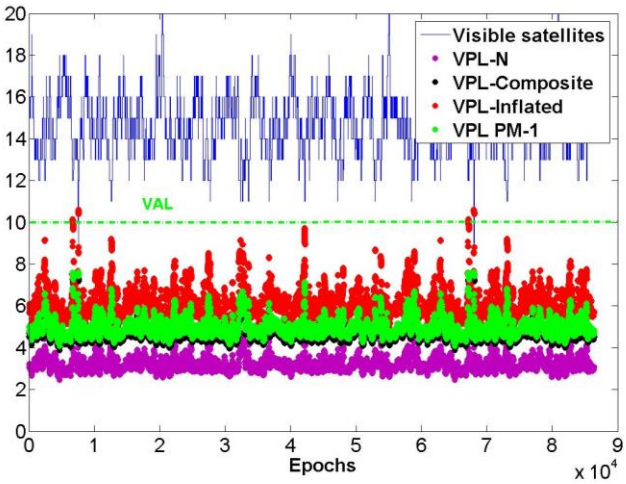

Figure 9-VPLs with D_{TH}=5km for GPS + GAL constellations

In the GPS and Galileo constellations case, the same conclusions can be made as in the GPS case presented before and inequalities (16) and (17) are still verified.

The difference between $VPL_{inflated}$ (red line) and VPL_{PM1} (green line) is more important and the VPL_{PM1} is closer to $VPL_{Composite}$ (black line) compared to the GPS case presented in Figure 8.

By analyzing these results and because we found VPLs closer to the black line representing $VPL_{Composite}$, the conclusion that the new methodology to bound non-nominal troposphere provides a better availability and keeps the integrity ensured is made.

However, this methodology requires also to send 18 parameters (μ_{max}).In order to reduce the number of parameters, this methodology was modified by fitting the curve representing the μ_{max} over elevations by a "bounding" curve always above μ_{max}. The following equation was found and verified this condition:

$$\mu_{max}(i) = 1.31 \times \exp\left(-\frac{Elev(i)}{14.21}\right) + 0.28 \qquad (18)$$

Where $Elev(i)$ represents the elevation of the satellite i in degrees.

The Figure 10 represents μ_{max} over elevations for both new methodologies: with the 18 parameters sent and with the equation (18).

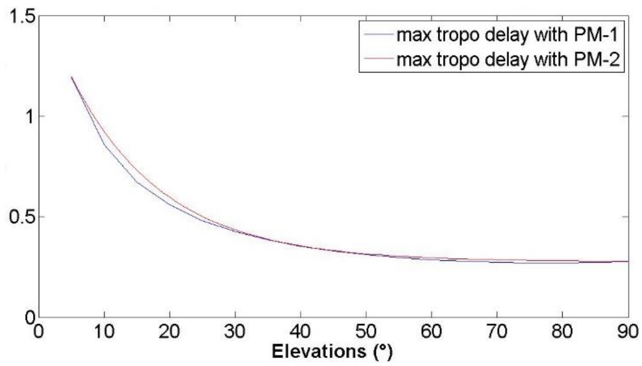

Figure 10 -μ_{max} with the 2 new methodologies

Then, a new VPL named VPL_{PM2} based on calculation of μ_{max} according to (18) is represented in the same figure as the Figure 8 and Figure 9 in order to compare performance results.

In the following Figure 11, the different VPLs presented above are represented for the GPS constellation with a distance from ground station to runway threshold (D_{TH}) of 5km and VPL_{PM2} is designated by the yellow curve.

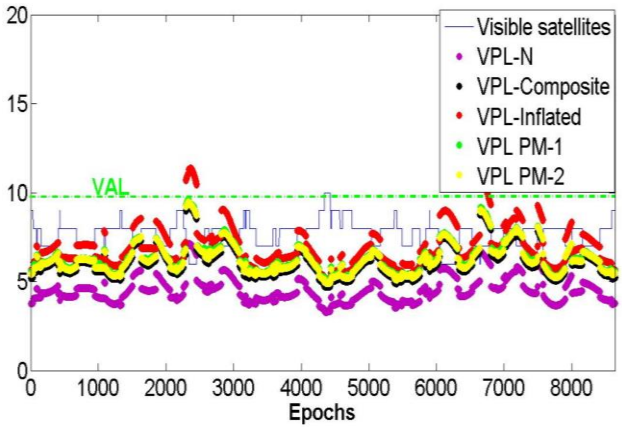

Figure 11- VPLs with D_{TH}=5km for GPS constellation only

By analyzing the previous Figure 11, the following inequality between the VPL_{PM1} represented by the green line and VPL_{PM2} represented by the yellow line is verified:

$$VPL_{PM2} \leq VPL_{PM1} \qquad (19)$$

That means that availability is improved although the difference between both data is quite small.

In the following Figure 12, the different VPLs presented above are represented for the GPS and Galileo constellations with a distance from ground station to runway threshold (D_{TH}) of 5km and VPL_{PM2} is designed by the yellow curve.

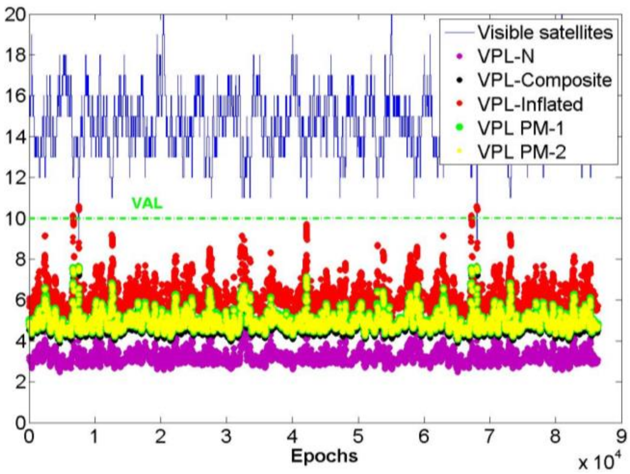

Figure 12 -VPLs with D_{TH}=5km for GPS + GAL constellations

In the previous Figure 12, the same conclusion as for Figure 11 is made.

Furthermore, although the difference between VPL_{PM2} and VPL_{PM1} is small, availability is improved and integrity is still ensured. But this new methodology with the "bounding" fitting is preferred because it requires lower data transmitted. Indeed, the equation (18) can be directly applied at the aircraft instead of sending 18 parameters what reduces the VDB transmission requirements.

To complete this analysis and in order to be less conservative, an improvement was achieved by applying conspiring biases only to the selected "Worst subset of satellites" at one side of the wall model and for the worst geometry possible. This was done by searching for the azimuth of the wall and thus subset Q where the value$\sum_{Q}|S_{vert} \times \mu_{max}|$ is maximum.

This subset is represented and explained in the following Figure 13 and Figure 14

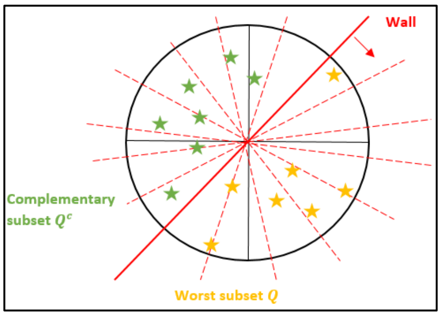

Figure 13 - Representation of the Worst subset Q

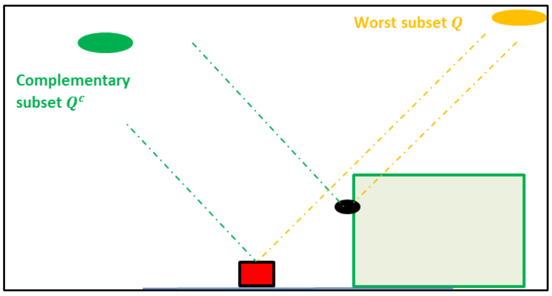

Figure 14- Representation of the Subset Q and the wall model

The new VPLs named $VPL_{Composite-b}$, VPL_{PM1-b} and VPL_{PM2-b} are computed in the same way as $VPL_{Composite}$, VPL_{PM1} and VPL_{PM2} respectively but based on subset Q.

In the Figure 15, the different VPLs presented above are represented for the GPS constellation with a distance from ground station to runway threshold (D_{TH}) of 5km. The new $VPL_{Composite-b}$, VPL_{PM1-b} and VPL_{PM2-b} are represented in black, light green and yellow respectively.

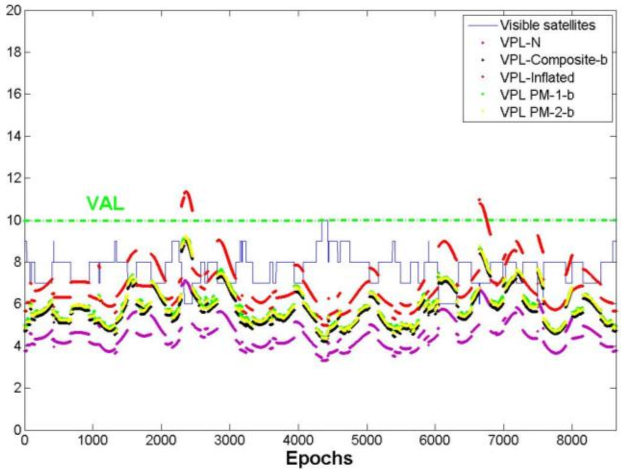

Figure 15 - VPLs with D_{TH}=5km for GPS constellation only

By analyzing the previous Figure 15 and by comparing with previous case represented in Figure 11, this new methodology implies a translation to the bottom of VPLs curves so in fact VPLs are reduced through this methodology except for $VPL_{Inflated}$ and VPL_N where this new methodology has no impact. Then as expected with less conservative assumptions, an improvement of the availability is observed.

In the Figure 16, the different VPLs introduced above are represented for the GPS and Galileo constellations with a distance from ground station to runway threshold (D_{TH}) of 5km. The new $VPL_{Composite-b}$, VPL_{PM1-b} and VPL_{PM2-b} are represented in black, light green and yellow respectively.

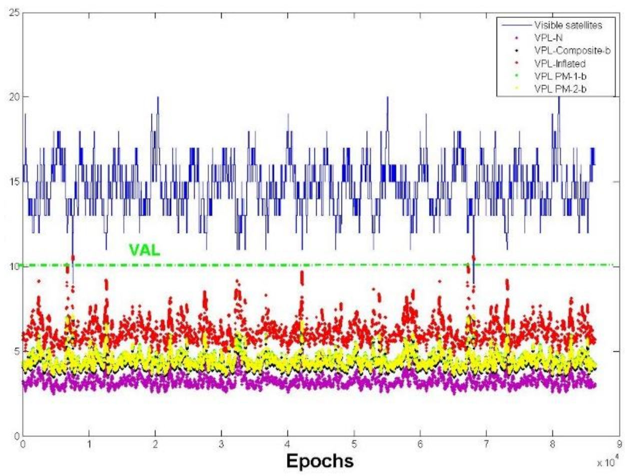

Figure 16- VPLs with D_{TH}=5km for GPS+GAL constellations

In the Figure 16, the same conclusion as for Figure 15 is made.

IONOSPHERE-FREE ANALYSIS

In case of DF GBAS, I-free smoothing may be used to eliminate the ionospheric delay term from the pseudorange observables and corrections. But as it is already mentioned above in the paper, the differential residual error due to the tropospheric delays has the same form as for SF case. It is expressed through the equation (1).

To complete this study, the same simulations were performed in the DF case with I-Free smoothing technique. Several analyses with different smoothing constants were realized but in this paper only results for 100s smoothing constant are presented.

To clarify figures, only results for the last presented methodology are analyzed in this paper.

In the Figure 17, $VPL_{Composite-b}$, VPL_{PM1-b} and VPL_{PM2-b} are represented in black, light green and yellow respectively, for the GPS constellation with a distance from ground station to runway threshold (D_{TH}) of 5km.

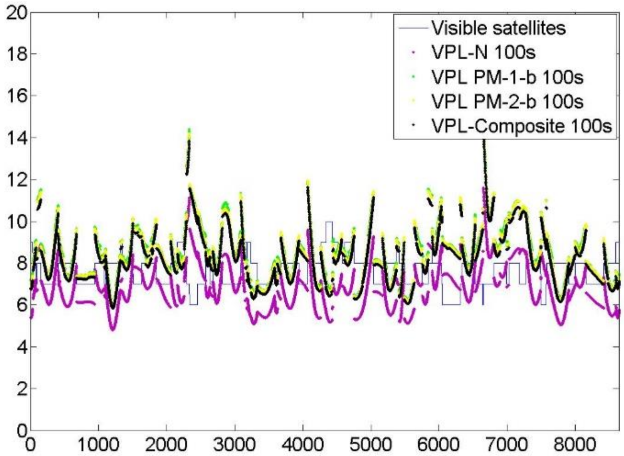

Figure 17- VPLs for I-free case with 100s smoothing constant with D_{TH}=5km for GPS constellation only

By analyzing the previous Figure 17, integrity seems to be ensured because the following inequality is verified:

$$VPL_{Composite} \leq VPL_{PM1-b} \leq VPL_{PM2-b} \qquad (20)$$

In the following Figure 18, $VPL_{Composite-b}$, VPL_{PM1-b} and VPL_{PM2-b} are represented in black, light green and yellow respectively, for the GPS and Galileo constellations with a distance from ground station to runway threshold (D_{TH}) of 5km.

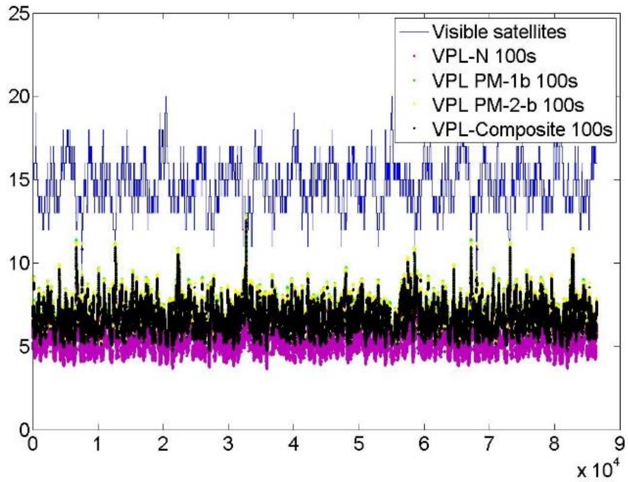

Figure 18 - VPLs for I-free case with 100s smoothing constant with D_{TH}=5km for GPS+GAL constellations

In the previous Figure 18, the same conclusion as for Figure 17 is made.

These results show that these new methodologies are still applicable in the DF case by applying the I-Free smoothing technique.

SUMMARY

The results presented with the existing methodology show a significant inflation of the VPLs in order to bound the non-nominal troposphere using the methodology proposed by Ohio University. However, this is the simplest solution to implement given the GAST C/D message definition. It appears excessively conservative to apply this bound. Thus, further investigation is needed on the appropriate model to be taken.

Furthermore, in all cases, there is a notable difference between the $VPL_{inflated}$ represented by the red curve and the $VPL_{Composite}$ represented by black curve. This difference is larger in the dual-constellation case than in the case where only the GPS constellation is used. Furthermore, with a larger D_{TH}, a greater difference between curves can also be observed.

In order to meet the requirements for the worst performing aircraft, lower VALs may be required. It is important to note that at some epochs VPL inflated is above the VAL of 10m. Clearly with lower VALs, availability could be impacted. Under such conditions, it would be beneficial to utilize a tropospheric bounding methodology which leads to VPLs closer to the black line (according figures plotted above in this paper).

That is why the last part of this paper deals with a new methodology which seems to improve the performance by having a better availability than with the existing methodology and this by keeping integrity ensured. This new methodology which can be also used in the DF case with I-free smoothing technique, can be seen as a “low data transmitted” solution which was a main issue in this study.

This paper has initiated the process of assessing the impact of modelling the non-nominal troposphere on GBAS VPLs.

The next steps of this study should include:

- Analyzing European meteorological data within the associated task in the SESAR WP15.3.7
- Using these data to better select and parameterize the threat model for the European region and so to reassess the choice of model and the model parameterization.

These tasks should be performed by using 3D Numerical Weather Models (NWM) such as HARMONIE provided by KNMI (Royal Netherland Meteorological Institute) and AROME provided by Meteo France. Both models are Non-Hydrostatic Models and are usually used for weather forecasting and analysis. They have a 2.5 km horizontal resolution and counts 60 vertical levels. HARMONIE which runs 4 previsions per day and 8 update analysis per day (3-hourly), covers an area around Netherland and AROME which as 5 previsions per day and 8 update analysis per day covers an area around France.
Data extracted from these models could be used to complete our analysis.

Then further works could be realized for:

- Developing a low data solution to compute a closer bound in the protection level domain, and investigate if it is possible, without modification of the VPL computation at the Aircraft side.
- Examining a greater range of D_{TH} such as 7, 8 or 10km should be realized in view of future constraint relaxations concerning the maximum value of D_{TH} as proposed by NSP in [4].

ACKNOWLEDGMENTS

The author would like to thanks the DSNA and NLR and more particularly Pierre Ladoux and Henk Veerman for their help and advice during this work. Also the author wants to thanks all partners of the SESAR WP 15.3.7.

REFERENCES

[1] D. W. Diggle, "An investigation into the use of Satellite Based positioning systems for flight reference/autoland operations," Ohio, 1994.

[2] F. Van Graas, V. Krishnan, R. Suddapalli and T. Skidmore, "Conspiring Biases in the LAAS," in *ION 60th Annual Meeting/U.S Air force institute os Technology & the U.S Air force Research Laboratory*, Dayton,OH, 2004.

[3] F. Van Graas and Z. Zhu, "Tropospheric Delay Threats for the GBAS," in *ITM of the ION*, San Diego, CA, 2011.

[4] A. F. Ken, J. Mcdonald and B. Johnson, "ICAO/NSP/WGW WP16, Observed Nominal Atmospheric Behavior using honeywell's GAST D Ionosphere Gradient Monitor, CSG meeting," Montreal, 2014.

[5] B. Pervan, S. Pullen and I. Sayim, "Sigma etimation, Inflation and Monitoring in the LAAS Ground System," in *ION GPS 2000*, Salt lake city, 2000.

[6] J. Seo, J. Lee, S. Pullen, P. Enge and S. Close, "Targeted Parameter Inflation within GBAS to minimize anomalous Ionospheric Impact," *Journal of aircraft*, vol. 49, no. 2, p. 587, 2012.

[7] J. Rife and S. Pullen, "The Impact of Measurement Biases on Availability for CAT III LAAS," in *ION*, 2005.

[8] A. Guilbert, C. Milner and C. Macabiau, "Optimal Processing Scheme for meeting CAT II/III with MC/MF GBAS," in *NAVITEC 2014*, ESA/ESTEC - Noordwijk - The Netehrlands, 2014.

[9] RTCA Inc., Minimum Operational Performance Standards (MOPS) for GPS Local Area Augmentation System (LAAS) Airborne Equipment - RTCA DO-253C, Washington DC, 2008.

[10] *"Private Correspondence" between Ohio University and Other Partners*, 2014.

[11] G. Xu, GPS Theory, Algorithms and Applications, Springer, 2007.

[12] NSP working group, GBAS CAT II/III Development Baseline SARPs, 2010.

APPENDIX

<u>For D_{TH} = 5km</u>

For GPS constellation with N=6

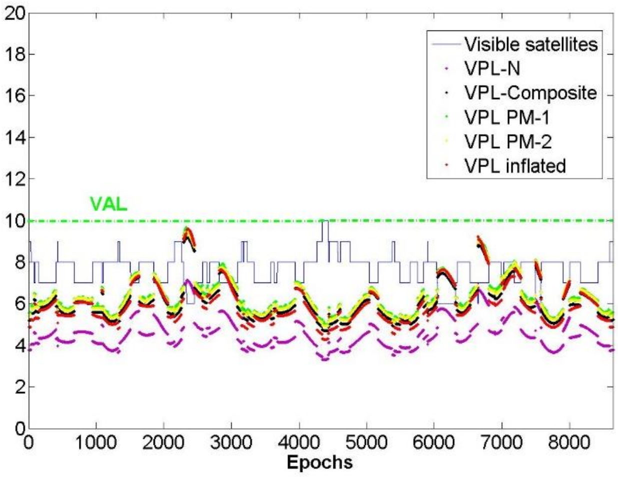

For GPS+GAL constellations with N=12

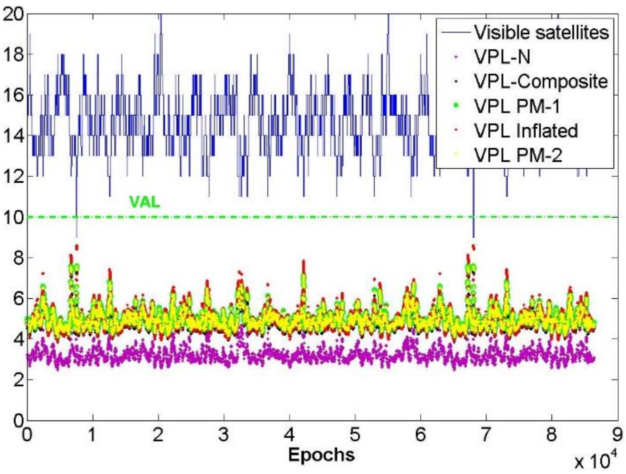

<u>For D_{TH} = 10km</u>

For GPS constellation with N=6

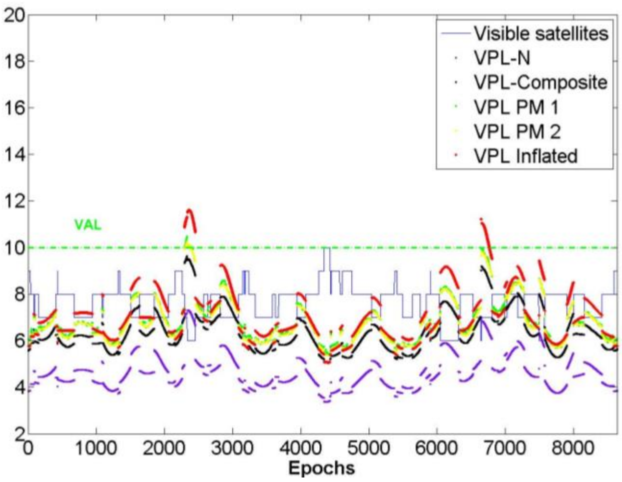

For GPS+GAL constellations with N=12